National Renewable Energy Laboratory
A national laboratory of the U.S. Department of Energy
Office of Energy Efficiency & Renewable Energy
Innovation for Our Energy Future

Characterization of 19.9%-Efficient CIGS Absorbers

Preprint

I. Repins, M. Contreras, M. Romero, Y. Yan, W. Metzger, J. Li, S. Johnston, B. Egaas, C. DeHart, and J. Scharf
National Renewable Energy Laboratory

B.E. McCandless
Institute for Energy Conversion

R. Noufi
Solopower

Presented at the 33rd IEEE Photovoltaic Specialists Conference
San Diego, California
May 11–16, 2008

Conference Paper
NREL/CP-520-42539
May 2008

NREL is operated by Midwest Research Institute • Battelle Contract No. DE-AC36-99-GO10337

NOTICE

The submitted manuscript has been offered by an employee of the Midwest Research Institute (MRI), a contractor of the US Government under Contract No. DE-AC36-99GO10337. Accordingly, the US Government and MRI retain a nonexclusive royalty-free license to publish or reproduce the published form of this contribution, or allow others to do so, for US Government purposes.

This report was prepared as an account of work sponsored by an agency of the United States government. Neither the United States government nor any agency thereof, nor any of their employees, makes any warranty, express or implied, or assumes any legal liability or responsibility for the accuracy, completeness, or usefulness of any information, apparatus, product, or process disclosed, or represents that its use would not infringe privately owned rights. Reference herein to any specific commercial product, process, or service by trade name, trademark, manufacturer, or otherwise does not necessarily constitute or imply its endorsement, recommendation, or favoring by the United States government or any agency thereof. The views and opinions of authors expressed herein do not necessarily state or reflect those of the United States government or any agency thereof.

Available electronically at http://www.osti.gov/bridge

Available for a processing fee to U.S. Department of Energy and its contractors, in paper, from:

U.S. Department of Energy
Office of Scientific and Technical Information
P.O. Box 62
Oak Ridge, TN 37831-0062
phone: 865.576.8401
fax: 865.576.5728
email: mailto:reports@adonis.osti.gov

Available for sale to the public, in paper, from:

U.S. Department of Commerce
National Technical Information Service
5285 Port Royal Road
Springfield, VA 22161
phone: 800.553.6847
fax: 703.605.6900
email: orders@ntis.fedworld.gov
online ordering: http://www.ntis.gov/ordering.htm


Printed on paper containing at least 50% wastepaper, including 20% postconsumer waste

CHARACTERIZATION OF 19.9%-EFFICIENT CIGS ABSORBERS

Ingrid Repins,[1] Miguel Contreras,[1] Manuel Romero,[1] Yanfa Yan,[1] Wyatt Metzger,[1] Jian Li,[1] Steve Johnston,[1]
Brian Egaas,[1] Clay DeHart,[1] John Scharf,[1] Brian E. McCandless,[2] and Rommel Noufi[3]
[1]National Renewable Energy Laboratory, Golden, CO 80401
[2]Institute for Energy Conversion, Newark, DE 19716
[3]Solopower, San Jose, CA 95138

ABSTRACT

We recently reported a new record total-area efficiency, 19.9%, for $CuInGaSe_2$ (CIGS)-based thin-film solar cells [1]. Current-voltage analysis indicates that improved performance in the record device is due to reduced recombination. The reduced recombination was achieved by terminating the processing with a Ga-poor (In-rich) layer, which has led to a number of devices exceeding the prior (19.5%) efficiency record. This paper documents the properties of the high-efficiency CIGS by a variety of characterization techniques, with an emphasis on identifying near-surface properties associated with the modified processing.

INTRODUCTION

Understanding the physical mechanisms that lead to champion CIGS devices is important for a number of reasons. First, this understanding helps define a pathway to future performance improvements. It also helps identify performance sensitivities that can improve yield and efficiency for CIGS devices deposited by related industrial techniques.

In this paper, we document the properties of high-efficiency (19.9%) CIGS by a variety of characterization techniques, with an emphasis on identifying near-surface properties associated with the modified processing.

FILM GROWTH AND DEVICE PERFORMANCE

The standard device layers and the processing used in the record CIGS devices have been described elsewhere [2,3,4,5,6]. The processing change responsible for the recent 0.4% (absolute) efficiency improvement is the termination of the three-stage process without Ga for the last ~100 Å of deposition. This modified termination is illustrated in Figure 1, which shows the In and Ga rates as measured by electron emission impact spectroscopy at the end of the three-stage CIGS deposition. Instead of maintaining the atomic ratio Ga/(In+Ga)~0.3 as throughout the rest of the deposition, about 30 Å of In (resulting in ~100 Å of chalcopyrite) is deposited without Ga at the end of the deposition.

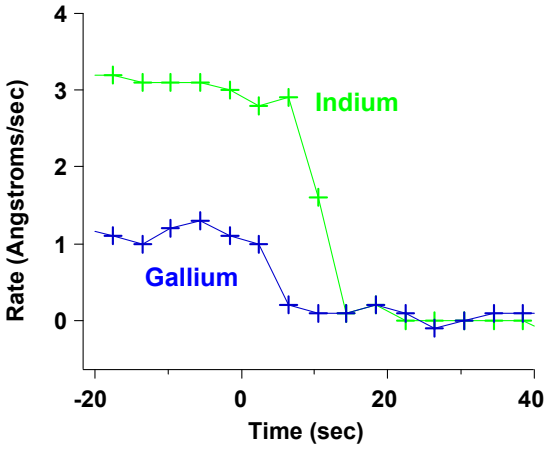

Figure 1: In and Ga rates at the end of three-stage CIGS deposition process for 19.9%-efficient device. Zero-rate background signal has been removed.

The processing variation illustrated in Figure 1 has led to the fabrication of a number of devices exceeding the previous efficiency record, 19.5% for a 0.42-cm^2 device [7]. Improved devices have been demonstrated in more than one evaporator and by several operators. The repetition of improved results is summarized in Table 1, which lists devices exceeding the previous efficiency records. Shown are the device name, device area, efficiency (η), open-circuit voltage (V_{oc}), fill factor (FF), and short-circuit current density (J_{sc}). The column in Table 1 titled "Official Measurement?" is listed as "Yes" for current density-voltage (J-V) measurements made by the National Renewable Energy Laboratory (NREL) Device Performance Group [8]. This column is listed as "No" for J-V measurements performed at the NREL thin-film group user facility.

Table 1: Summary of devices made using modified processing termination with performance exceeding prior record values for 0.42- and 1-cm^2 devices.

Device Name	Area (cm^2)	η (%)	V_{oc} (mV)	FF (%)	J_{sc} (mA/cm^2)	Official Measurement?
M2992-11#5	0.419	19.9	690	81.2	35.4	Yes
C2183-12#5	0.416	19.9	697	80.0	35.7	Yes
C2219-21#7	0.417	19.8	714	79.1	35.1	Yes
M2992-11#4	0.419	19.7	690	81.2	35.1	Yes
M2992-11#6	0.419	19.7	690	81.1	35.3	Yes
C2183-12#4	0.417	19.7	695	80.0	35.5	Yes
C2200-22#1	0.420	19.6	725	80.6	33.6	No
C2213-22#2	**0.994**	19.2	716	80.4	33.4	Yes

MATERIALS CHARACTERIZATION

Two features of the high-efficiency material are of particular interest: reduced recombination, and the effect of the Ga-poor process termination on the surface layer. We examined these features using grazing-incidence X-ray diffraction (GIXRD), time-resolved photoluminescence (TRPL), transmission electron microscopy (TEM), energy-dispersive spectroscopy (EDS), capacitance-voltage (CV) profiling, scanning tunneling luminescence spectroscopy (STL), and cathodoluminescence (CL) spectrum imaging.

STL and CL

We modified a scanning tunneling microscope at NREL to map STL in conjunction with CL [9]. The estimated penetration depth for tunneling electrons used to excite luminescence during STL measurements is estimated to be no more than 50 nm [10]. On the other hand, the 15-keV electrons used to excite luminescence during CL measurements are estimated to penetrate about 1 μm into the film. Thus, the STL probes the film very near the surface, whereas the CL probes into the bulk of the film. The luminescence from 19.9%-efficient CIGS was characterized in terms of excitation source (CL vs. STL) and position. These data were compared with earlier data on 13%- and 19.5%-efficient CIGS.

When room-temperature CL mapping is performed, the 19.9%-efficient CIGS exhibits a 5%–10% reduction in luminescence intensity at the grain boundaries, compared to the grain interiors. This magnitude of intensity loss is typical of devices with efficiency greater than 18%. Lower-efficiency devices exhibit more nonradiative recombination (20%–30% intensity loss) at the grain boundaries. Scanning electron microscope (SEM) plan views and the corresponding CL intensity maps are shown in Figure 2 for 19.9%- and 13%-efficient absorbers.

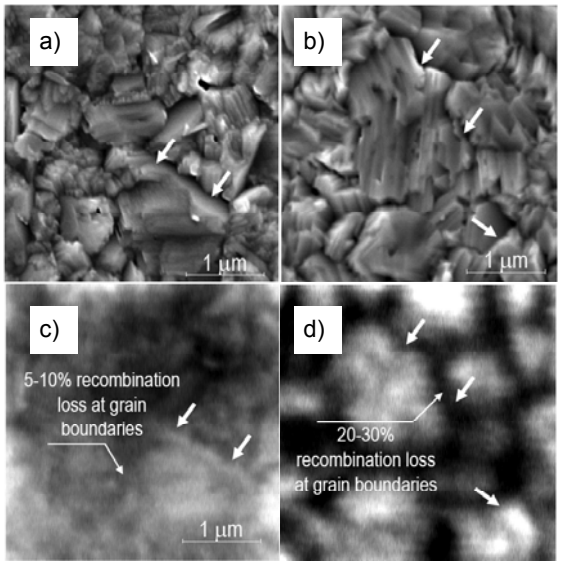

Figure 2: SEM plan view of a) 19.9%- and b) 13%-efficient CIGS. Corresponding CL maps for c) 19.9%- and d) 13%-efficient CIGS.

STL, however, reveals a difference between the 19.9% device and all earlier material measured by this technique. Figure 3 compares a room-temperature CL spectrum from the 19.9% sample (pink), STL spectrum from the same point on the 19.9% sample (dark blue), STL spectrum from an 18% reference sample (yellow), and CL spectrum from the 18% reference sample (light blue). The reference sample exhibits the typical red shift between the CL and STL. Presumably, the red shift occurs because the surface of the CIGS contains a higher density of band-tailing defect states than the bulk. In the 19.9% sample, however, there is no red shift between the CL and STL. The lack of red shift implies that the material quality near the surface has been improved in the 19.9% material.

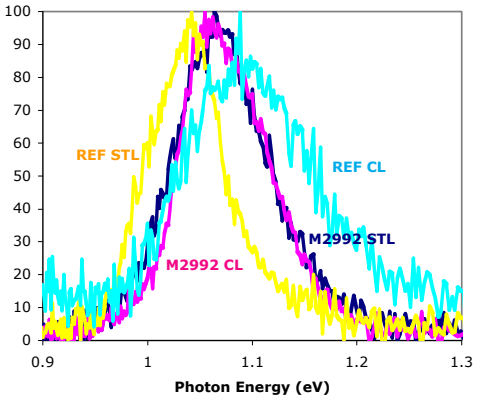

Figure 3: Comparison of cathodoluminescence spectrum from 19.9%-efficient sample (in pink), tunneling luminescence spectrum from 19.9% sample (dark blue), cathodoluminescence spectrum from 18% reference sample (light blue), and tunneling luminescence spectrum from 18% reference sample (yellow).

TEM

Earlier measurements at NREL on CIGS that produced 19.5%-efficient devices indicated nanodomains when examined with high-resolution TEM (HRTEM), high-angle annular dark-field (HAADF) images, and EDS [11]. Similar measurements on the new 19.9%-efficient material show less evidence of nanodomains. Figure 4a shows an atomic number (Z) contrast TEM image of the 19.9% CIGS. The interior of the film is at the upper left corner of the image, and vacuum appears as the dark area in the lower right corner. A small gradual change in brightness is seen across the sample, most likely due to a gradient in cleaved sample thickness and gradual composition change toward the surface. However, no nanodomains are visible. For contrast, Figure 4b shows the same type of image from the early 19.5%-efficient material. Nanoscale composition domains are clearly visible.

EDS data also indicate less pronounced nanodomains in the new material. In the 19.5%-efficient CIGS, Cu ratio (Cu/(In+Ga)) and Ga ratio (Ga/(In+Ga)) exhibit large fluctuations (~2x) when measured by EDS in 5-nm steps over 70 nm. The new data exhibit somewhat smaller variations in the Cu and Ga ratios (~1.5x). Figure 5a shows Cu and Ga ratios as measured by EDS. The electron-probe size is estimated to be about 5 Å. The system detection error bar is estimated to be ±2%.

Figure 5b is a TEM image that shows the path of the EDS measurements. The top of the red line corresponds to 0-nm displacement.

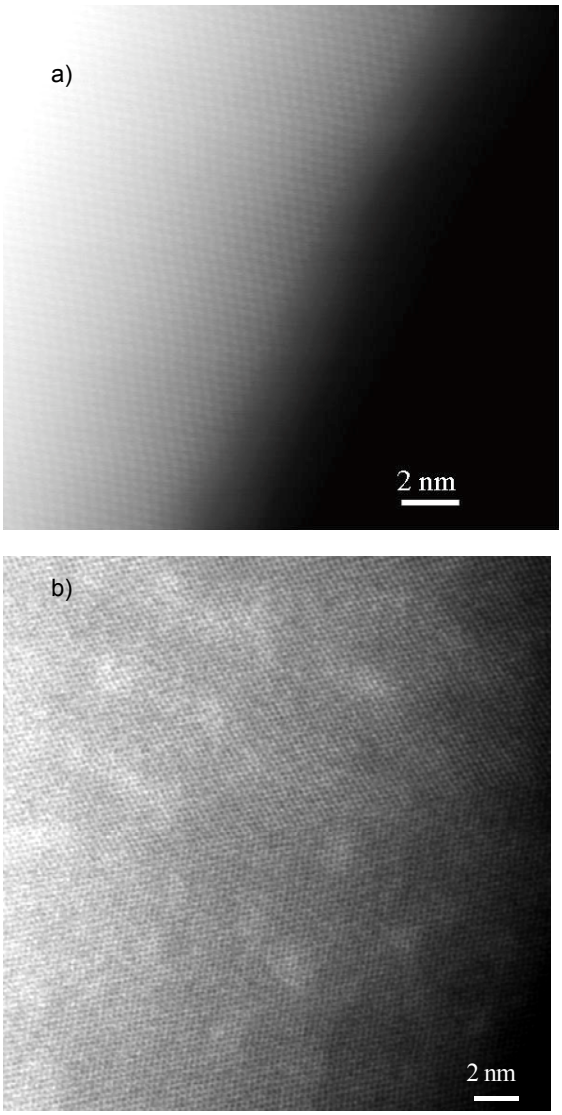

Figure 4: Z-contrast TEM image of a) 19.9%-efficient CIGS, and b) earlier 19.5%-efficient CIGS.

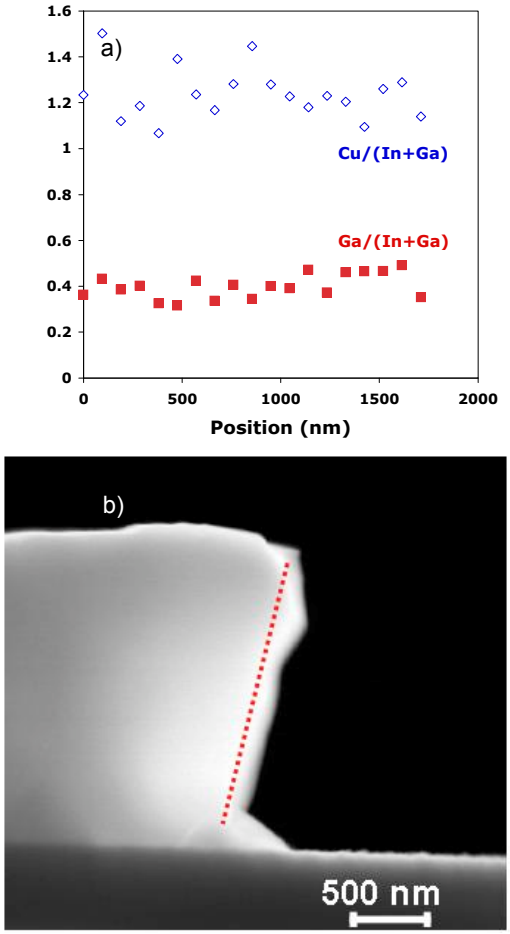

Figure 5: a) Composition as a function of position in the 19.9%-efficient CIGS, and b) TEM image showing the line along which these measurements were taken.

TRPL

Carrier lifetime was measured by TRPL, both on the CIGS film and the device. The measurement and analysis technique has been described elsewhere [12]. The lifetime measured in the 19.9%-efficient device, 5.5 ns, is somewhat longer than what has been measured on other devices. For example, Figure 6 shows efficiency versus lifetime for the record device, and for other recent samples made at NREL with variations in the Ga contents and composition profiles. The increased lifetime is consistent with improved diode quality factor in the device. However, one should not strictly associate the measured lifetime with reduced recombination, because several other factors—including charge separation in the depletion region, measurement intensity, and fitting algorithm—also influence the apparent lifetime value [13,14]. Furthermore, variations in measurement and analysis procedures from one study to the next preclude a straightforward comparison of the new results with many of those in the literature.

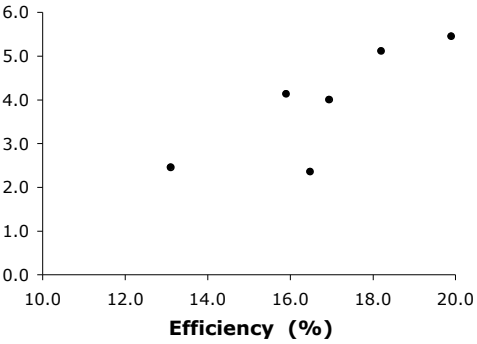

Figure 6: Efficiency versus lifetime measured in CIGS devices with a variety of Ga contents and composition gradings.

CV

CV measurements were used to examine carrier density. Data taken at 50 kHz are shown in Figure 7. Zero-bias depletion width is marked with a diamond. Capacitance as a function of frequency varied little in the range from 1 to 200 kHz. The maximum carrier density of about 2 x 10^{16} cm^{-3} and zero-bias depletion width less than 0.5 μm are typical of CIGS devices made at NREL with efficiencies greater than 19% [15]. Lower-efficiency devices made at NREL tend to have a slightly lower carrier density (≤1 x 10^{16} cm^{-3}) and slightly longer zero-bias depletion widths [12,16,17].

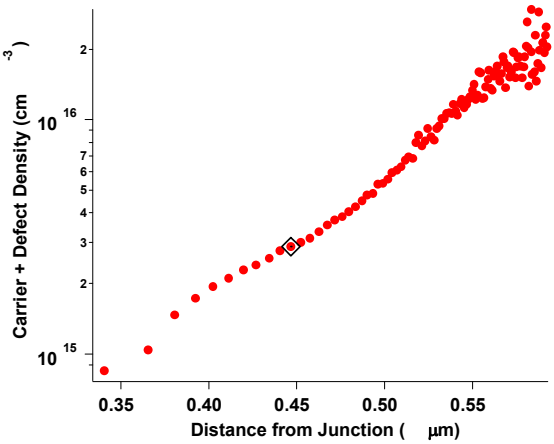

Figure 7: Carrier density versus distance from the junction as derived from CV profiling. The zero-bias depletion width is marked with a diamond.

GIXRD

GIXRD data were taken at the Institute for Energy Conversion (IEC). For incident angles from 0.5 to 4 degrees (estimated penetration depths of 0.13 to

1.0 μm), the (112) peak centered near 27 degrees shows the expected progression to lower values of 2Θ, due to decreasing Ga content as the incident beam penetrates the notched Ga profile [18]. Typical of high-efficiency devices, the peaks are relatively narrow. For example, the half width at half maximum of the (112) peak was measured at 0.166 degrees using a 4-degree incident angle. However, this narrow peak width does not distinguish the record material from other high-quality CIGS.

Low incident angles were used to probe the material structure as near as possible to the surface. GIXRD measurements at 0.25-degree incident angle should probe about 50 nm into the film. Such measurements were compared for the record sample, a sample made with the same recipe but terminating the process with Ga (opposite of what is shown in Figure 1), and a sample made without any intentional Ga grading. These samples exhibited nearly identical compositions when measured by EDS. GIXRD scans of the (112) peak for the three samples are shown in Figure 8. All samples show a peak centroid shift to angles significantly higher than that expected from the 0.36 Ga ratio measured by EDS. These peak shifts are not associated with the alignment of the diffractometer. To account for the peak shifts of Figure 8 by Ga content alone, the ratio Ga/(In+Ga) near the surface would need to be 0.46 for sample 34186, 0.60 for M2995, and 0.71 for M2992. Instead, it is likely that the peak shifts are due to decreased Cu content near the film surface [19] or to lattice strain. The 19.9%-efficient CIGS exhibits the largest peak shift.

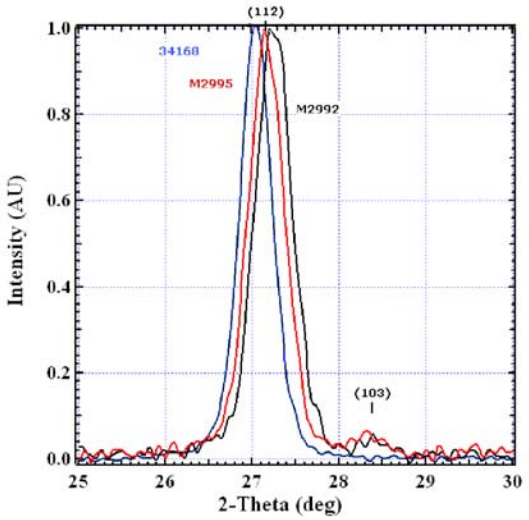

Figure 8: GIXRD (112) scans of 19.9%-efficient CIGS film (M2992, black), similar film with Ga process termination (M2995, red), and CIGS film without Ga grading (IEC 34168, blue).

CONCLUSIONS

A modification to the termination of the three-stage co-evaporation process has recently improved the performance of CIGS devices at NREL. We applied a variety of characterization techniques to the 19.9%-efficient CIGS. Several of the extracted properties are typical of CIGS with efficiency exceeding ~19%. These properties include carrier density around 2 x 10^{16} cm^{-3}, zero-bias depletion width just under 0.5 μm, a relatively long PL decay time on devices, relatively high luminescence intensity at the grain boundaries, and narrow GIXRD peaks. Other properties appear to be new to the improved material: absence of a red shift in the luminescence spectrum near the CIGS surface, diminished manifestation of nanodomains, and increased shifting of the GIXRD (112) peak to smaller lattice parameters.

ACKNOWLEDGEMENTS

This work was supported by the U.S. Department of Energy under Contract No. DE-AC36-99GO10337 with the National Renewable Energy Laboratory. The authors thank Craig L. Perkins and Bobby To for film composition data, the NREL Device Performance Group for J-V measurements, Falah Hasoon for discussions on film growth, and Tim Gessert and Ramesh Dhere for helpful review.

REFERENCES

[1] I. Repins, M.A. Contreras, B. Egaas, C. DeHart, J. Scharf, C.L. Perkins, B. To, and R. Noufi, 19.9% Efficient ZnO/CdS/$CuInGaSe_2$ Solar Cell with 81.2% Fill Factor, Accepted for *Progress in Photovoltaics*, 9 January 2008.

[2] K. Ramanathan, M.A. Contreras, C.L. Perkins, S. Asher, F.S. Hasoon, J. Keane, D. Young, M. Romero, W. Metzger, R. Noufi, J.S. Ward, and A. Duda, Properties of 19.2% efficiency ZnO/CdS/$CuInGaSe_2$, thin-film solar cells, *Progress in Photovoltaics Research and Applications* **11**, 2003, pp. 225–230.

[3] M.A. Contreras, B. Egaas, K. Ramanathan, J. Hiltner, A. Swartzlander, F. Hasoon, and R. Noufi, Progress toward 20% efficiency in Cu(In,Ga)Se_2 polycrystalline thin-film solar cells, *Progress in Photovoltaics Research and Applications* **7**, 1999, pp. 311–316.

[4] U.S. Patent No. 5,441,897 (August 15, 1995) and U.S. Patent No. 5,436,204 (July 25, 1995).

[5] M.A. Contreras, J.R. Tuttle, A. Gabor, A. Tennant, K. Ramanathan, S. Asher, A. Franz, J. Keane, L. Wang, J. Scofield, and R. Noufi, High efficiency Cu(In,Ga)Se_2-based solar cells:

Processing of novel absorber structures. *Conference Record of the 24th IEEE Photovoltaics Specialists Conference,* 1994, pp. 68–75.

[6] M.A. Contreras, M.J. Romero, B. To, F. Hasoon, R. Noufi, S. Ward, and K. Ramanathan. Optimization of CBD CdS process in high-efficiency Cu(In,Ga)Se_2-based solar cells, *Thin Solid Films* **403**–**404**, 2002, pp. 204–211.

[7] M.A. Contreras, K. Ramanathan, J. Abushama, F. Hasoon, D.L. Young, B. Egaas, and R. Noufi, Diode characteristics in state-of-the-art ZnO/CdS/Cu($In_{1-x}Ga_x$)Se_2 solar cells, *Progress in Photovoltaics* **13**, 2005, pp. 209–216.

[8] See, for example, http://www.nrel.gov/pv/measurements/device_performance.html

[9] M.J. Romero, C.S. Jiang, M.M. Al-Jassim, and R. Noufi, Scanning tunneling luminescence of grain boundaries in Cu(In,Ga)Se_2, *Proceedings of the 2004 DOE Solar Energy Technologies Program Review Meeting*, 2004, NREL/CP-520-36975.

[10] M.J. Romero, C.S. Jiang, R. Noufi, and M. Al-Jassim, Photon emission in $CuInSe_2$ thin films observed by scanning tunneling microscopy, *Applied Physics Letters* **86**, 2005, 143115.

[11] Y. Yan, R. Noufi, K.M. Jones, K. Ramanathan, M.M. Al-Jassim, and B.J. Stanbery, Chemical fluctuation-induced nanodomains in Cu(In,Ga)Se_2 films, *Applied Physics Letters* **87**, 2005, 121904.

[12] I.L. Repins, B.J. Stanbery, D.L. Young, S.S. Li, W.K. Metzger, C.L. Perkins, W.N. Shafarman, M.E. Beck, L. Chen, V.K. Kapur, D. Tarrant, M.D. Gonzalez, D.G. Jensen, T.J. Anderson, X. Wang, L.L. Kerr, B. Keyes, S. Asher, A. Delahoy, and B. von Roedern, Comparison of device performance and measured transport parameters in widely-varying Cu(In,Ga)(Se,S) solar cells, *Progress in Photovoltaics* **14**, 2006, pp. 25–43.

[13] W.K. Metzger, I.L. Repins, and M. Contreras, Long recombination lifetimes in high-efficiency Cu(In,Ga)Se_2 solar cells, Submitted to *Applied Physics Letters*, April 2008.

[14] W.K. Metzger *et al*., *E-MRS 2008 Spring Meeting*, May 2008.

[15] R.N. Bhattacharya, M.A. Contreras, B. Egaas, and R.N. Noufi, High efficiency thin-film $CuIn_{1-x}Ga_xSe_2$ photovoltaic cells using a $Cd_{1-x}Zn_xS$ buffer layer, *Applied Physics Letters* **89**, 2006, 253503.

[16] R.N. Bhattacharya, J.F. Hiltner, W. Batchelor, M.A. Conteras, R.N. Noufi, and J.R. Sites, 15.4% $CuIn_{1-x}Ga_xSe_2$-based photovoltaic cells from solution-based precursor films, *Thin Solid Films* **361-362**, 2000, pp. 396–399.

[17] P.K. Johnson, J.T. Heath, J.D. Cohen, K. Ramanathan, and J.R. Sites, A comparative study of defect states in evaporated and selenized CIGS(S) solar cells, *Progress in Photovoltaics* **13**, 2005, pp. 579–586.

[18] B.E. McCandless, "Glancing incidence X-ray diffraction of polycrystalline thin films, *Materials Research Society* **865**, 2005, F4.1.1.

[19] I.M. Kotschau and H.W. Schock, Depth profile of the lattice constant of the Cu-poor surface layer in $(Cu_2Se)_{1-x}(In_2Se_3)_x$ evidenced by grazing incidence X-ray diffraction, *Journal of Physics and Chemistry of Solids* **64**, 2003, pp. 1559–1563.

REPORT DOCUMENTATION PAGE

Form Approved
OMB No. 0704-0188

The public reporting burden for this collection of information is estimated to average 1 hour per response, including the time for reviewing instructions, searching existing data sources, gathering and maintaining the data needed, and completing and reviewing the collection of information. Send comments regarding this burden estimate or any other aspect of this collection of information, including suggestions for reducing the burden, to Department of Defense, Executive Services and Communications Directorate (0704-0188). Respondents should be aware that notwithstanding any other provision of law, no person shall be subject to any penalty for failing to comply with a collection of information if it does not display a currently valid OMB control number.

PLEASE DO NOT RETURN YOUR FORM TO THE ABOVE ORGANIZATION.

1. REPORT DATE *(DD-MM-YYYY)*	2. REPORT TYPE	3. DATES COVERED *(From - To)*
May 2008	Conference Paper	11-16 May 2008

4. TITLE AND SUBTITLE
Characterization of 19.9%-Efficient CIGS Absorbers: Preprint

5a. CONTRACT NUMBER
DE-AC36-99-GO10337

5b. GRANT NUMBER

5c. PROGRAM ELEMENT NUMBER

6. AUTHOR(S)
I. Repins, M. Contreras, M. Romero, Y. Yan, W. Metzger, J. Li, S. Johnston, B. Egaas, C. DeHart, J. Scharf, B.E. McCandless, and R. Noufi

5d. PROJECT NUMBER
NREL/CP-520-42539

5e. TASK NUMBER
PVA74301

5f. WORK UNIT NUMBER

7. PERFORMING ORGANIZATION NAME(S) AND ADDRESS(ES)
National Renewable Energy Laboratory
1617 Cole Blvd.
Golden, CO 80401-3393

8. PERFORMING ORGANIZATION REPORT NUMBER
NREL/CP-520-42539

9. SPONSORING/MONITORING AGENCY NAME(S) AND ADDRESS(ES)

10. SPONSOR/MONITOR'S ACRONYM(S)
NREL

11. SPONSORING/MONITORING AGENCY REPORT NUMBER

12. DISTRIBUTION AVAILABILITY STATEMENT
National Technical Information Service
U.S. Department of Commerce
5285 Port Royal Road
Springfield, VA 22161

13. SUPPLEMENTARY NOTES

14. ABSTRACT *(Maximum 200 Words)*
We recently reported a new record total-area efficiency, 19.9%, for CuInGaSe2 (CIGS)-based thin-film solar cells. Current-voltage analysis indicates that improved performance in the record device is due to reduced recombination. The reduced recombination was achieved by terminating the processing with a Ga-poor (In-rich) layer, which has led to a number of devices exceeding the prior (19.5%) efficiency record. This paper documents the properties of the world-record-efficiency CIGS solar cell by a variety of characterization techniques, with an emphasis on identifying near-surface properties associated with the modified processing.

15. SUBJECT TERMS
CIGS; PV; record efficiency; thin film; solar cells; current-voltage; open-circuit voltage; fill factor; grazing-incidence X-ray diffraction;

16. SECURITY CLASSIFICATION OF:			17. LIMITATION OF ABSTRACT	18. NUMBER OF PAGES	19a. NAME OF RESPONSIBLE PERSON
a. REPORT	b. ABSTRACT	c. THIS PAGE			19b. TELEPHONE NUMBER (*Include area code*)
Unclassified	Unclassified	Unclassified	UL		

Standard Form 298 (Rev. 8/98)
Prescribed by ANSI Std. Z39.18